Centrifuge Simulations of the Interaction Between Folding, Faulting and Diapirism During Regional Extension

Elena Konstantinovskaya*
INRS-ETE, Québec, QC

Lyal Harris, Benjamin Carlier, Audrey Lessard-Fontaine, Jimmy Poulin and Adrien Handschuh
INRS-ETE, Québec, QC, Canada
lyal _harris@ete.inrs.ca

Eric L. Johnson and Nichola Thomas
Hartwick College, Oneonta, NY, United States

and

Sylvie Daniel
Université Laval, Québec, QC, Canada

Summary

Centrifuge modelling is shown to be a powerful technique for simulating (i) the interaction between faults and diapirs during rifting, (ii) the geometry of diapir-related folds, including sub-diapir structures, (iii) active folding associated with displacement on normal faults, and (iv) folds and faults related to gravitational collapse between lateral ramps in deltas. X-Ray computed tomography (CT scanning) and gOcad visualization permit the progressive 3D development of structures in centrifuge models to be studied. In aiding the interpretation of seismic and field data and providing a means of developing and testing structural hypotheses, centrifuge modelling can provide a valuable addition to a petroleum exploration program.

Introduction

Through investigating the behaviour of rheologically and dynamically similar systems, physical (analogue) models provide a better understanding of the progressive development and 3D geometry of structures in sedimentary basins and fold-thrust belts. Whilst sandbox models replicate brittle, upper crustal deformation, simulations using a high-acceleration centrifuge are often better suited to study dynamic systems where body forces (e.g. due to density differences) are important, or where active folding due to rheological contrasts between layers is significant. A pilot study was undertaken to develop new modelling materials and CT scanning techniques to simulate the interaction between diapirs and faults and the 3D geometry of structures in rift basins, deltas and passive margins through centrifuge analogue modelling.

Method

In diapir models, thin layers and "micro-laminates" of modelling clays and modelling clay-silicone putty mixes were used to simulate a sequence of inter-bedded sedimentary strata. Less dense/more ductile silicones simulating mobile salt horizons were placed at different levels in some models. The rheology and X-Ray properties of these modeling materials were quantified, and the ability to distinguish individual layers in multilayer packages through X-Ray computed tomography ("CT scanning") established. Prescribed cuts in some models represented fault planes of pre-determined initial dip and /or orientation (e.g. Fig. 1a). Other models comprising layer packages of different thickness and composition *without* initial structures were used to test the effects of lithology on deformation and diapir formation. In models of collapse structures between lateral ramps in deltas, layers were constructed between fixed wooded walls representing basement-controlled lateral ramps of differing geometry (Fig. 1b). Upper layers overlaid the entire wooden base. All models were placed in a rotor with layers vertical (Fig. 1c) and allowed to extend along one axis whilst undergoing an acceleration of ca. 950 G normal to the initial layering. CT scanning of models was performed at successive stages of their deformation and final models were serially sliced. Reconstructions of the 3D geometry of diapir margins, marker horizons, and faults in gOcad from digitised serial CT scans (e.g. Fig. 2) enabled the progressive development of models to be studied. Optimum CT scanner configurations and methodologies for scanning silicone-modelling clay layers were developed.


(a) (b) (c)
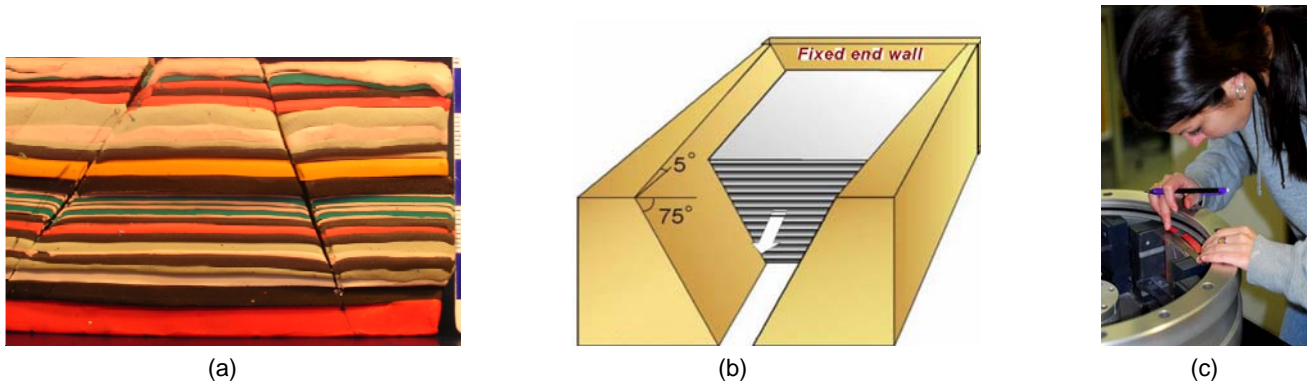
Figure 1: (a) Example of multilayered model prior to deformation where prescribed cuts represent faults. (b) Schematic diagram of lateral ramp models. Basal multilayers of modelling clay, silicone putty and modelling clay-silicone mixes were positioned between fixed wooden walls representing lateral ramps. Upper layers covered the entire base. (c) Models are positioned in the centrifuge rotor with layers vertical so that G forces act normal to initial layering.

Examples

(i) Diapir emplacement during extensional faulting. Displacement initially occurred on prescribed faults. Synthetic and antithetic listric normal faults that soled out on ductile horizons subsequently developed. Diapirs preferentially intruded normal faults, deforming fault planes and locally reversing fault dips leading to a termination of displacement on initial faults (Fig. 2). Model layers were folded producing domal culminations above diapirs and/or in the footwalls of normal faults. Broad synforms developed between normal faults of opposing dip and between diapirs. In models with a transfer fault deformation was compartmentalized: diapirs were better developed in the block that underwent less layer-parallel extension, and diapirs diverged away from the transfer fault and "walls" parallel but away from transfer faults (Fig. 2). Syn-extensional diapir models display many similarities with salt-related structures (e.g. Niger delta).
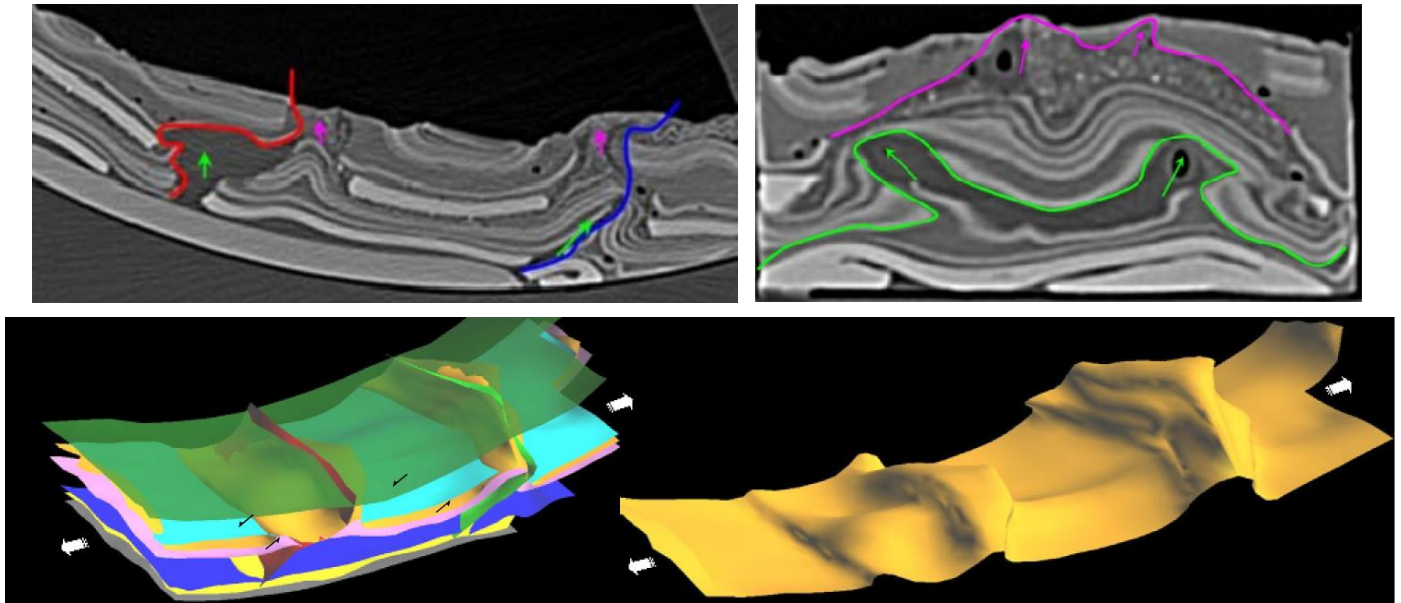
Figure 2: Top: CT scans parallel (left) and perpendicular (right) to the extension direction illustrate the geometry of silicone diapirs (tops in green and purple, right scan) and folds in adjacent intelayered modelling clay+silicone/silicone layers, and the deformation of early faults (red and blue). Bottom: gOcad reconstructions based on serial CT images of diapirs (gold) emplaced during dispacement on normal faults and a transfer fault.

(ii) The geometry of diapir-related folds, including sub-diapir structures. A variety of fold styles develop associated with diapir emplacement (Fig. 3). Recumbent isoclinal folds develop ajacent to the diapir trunk beneath the overhanging "tongue" of mushroom-shaped diapirs and tight to isoclinal upright to inclined synforms form between diapirs. Open domes form above diapirs. Models showed that layers *beneath* diapirs were also folded into broad antiforms, with associated parasitic folds in thinner layers. Viscous layers beneath synforms may thin/neck.
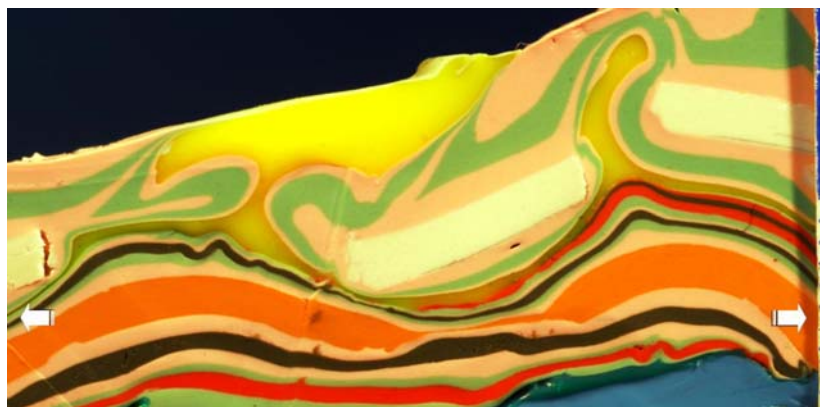
Figure 3: Fold styles in modelling clay+silicone and silicone (pink) layers associated with two stages in the development diapirs (less dense and more ductile, yellow silicone) during layer-parallel extension. Broad folds with minor parasitic folds develop *beneath* diapirs.

(iii) Folds associated with displacement on normal faults. Simple open folds develop in the footwall to extensional faults (Fig. 4 left). Tighter, more complex folds (Fig. 4 right) develop in footwall layers with strong mechanical anisotropy when competent dense horizons are displaced. Reverse drag

(upper layers, left), zero drag (lower layers, left) and normal drag (right) may occur in hangingwall layers depending on layer rheology and density.
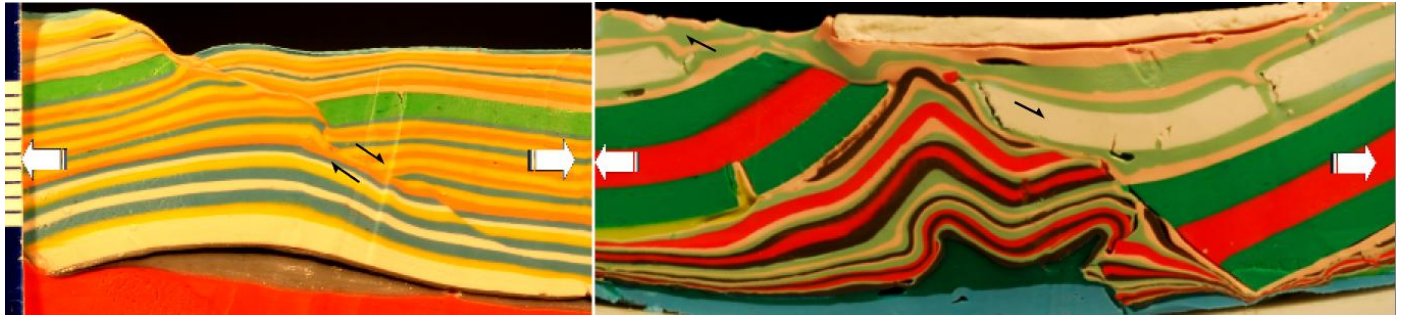

Figure 4: Folding of footwall and hanging wall layers during displacement on normal faults. The model at right comprises thick red and green competent and dense modelling clay layers, and lower modelling clay+silicone layers with a greater viscosity contrast in comparison to those in the left model. Ductile, less dense silicone (silver left, dark green right) separates basal and overlying layers.

(iv) Collapse between lateral ramps. A model of structures formed during collapse between convergent lateral ramps (Fig. 5) simulates structures that may form in deltas where basement structures localise transfer faults. Faults with normal and strike-slip components formed oblique to the extension direction in the areas adjacent to the fixed end wall and in the central part of the model. Folds with axes both perpendicular and parallel to the transport direction developed in the region closest to the moving end wall (equivalent to the delta toe area in nature) forming elongate domes and basins that fold isoclinal folds. Figure 5 illustrates the fine details of structures formed in "microlaminate" layers simulating interlayered sandstone and shales.

Figure 5: Oblique view of upper surface and vertical cut through a model simulating collapse between convergent lateral ramps showing changes from extensional to contractional deformation similar to that found in some deltas.

Conclusions

Centrifuge modelling is shown to be a powerful technique to simulate a variety of structures in rift basins, passive margins and deltas that canot be easily simulated in sandbox models, such as where diapirism and active folding of rheologically stratified sequences are important structural elements. Whilst results presented only illustrate structures formed in extensional settings, centrifuge modelling can equally well be applied to structures in contractional settings such as fold-

thrust belts. Model materials, CT scanning techniques, and image analysis software developed in this study allow fine details of structures to be developed and imaged and for 3D visualizations to be constructed in gOcad. Non-destructive visualization of models through CT scanning permits the progressive development of structures and superposed events to be studied. Centrifuge models aid interpretation of reflection seismic data and the determination of structural histories and deformation mechanisms in sedimentary basins.

Normal faults and/or fractures in competent horizons are shown to localise diapir intrusion then be subsequently deformed during diapir ascent. A variety of fold styles is associated with diapirs. Modelling results have implications for the study of sub-salt structures that represent important exploration targets in some basins (e.g. Gulf of Mexico) in being able to determine the geometry of folds *beneath* diapirs. Models illustrate folds formed during rifting or gravitational collapse that may otherwise have been interpreted as forming during regional shortening. The geometry of active folds in both the footwall and hangingwall of normal faults varies considerably for different layer rheologies and densities and complex folds may form where there are large rheological contrasts. Folds may develop with axes both perpendicular and parallel to the transport direction during collapse between convergent lateral ramps; similar structures may occur in deltas.

Acknowledgements